CIMAC CONGRESS 25
ZURICH, MAY 19 – 23, 2025

2025 | 417

A predictive energy management for hybrid ship propulsion system considering battery capacity decay

Electrification and Fuel Cells Development

chen chen, Harbin Engineering University

Liyun Fan, Harbin Engineering University
Zejun Jiang, Harbin Engineering University
Kui Xu, Harbin Engineering University
Quan Dong, Harbin Engineering University
Yunpeng Wei, Harbin Engineering University

ABSTRACT

The hybrid propulsion system (HPS), including various power sources, provides an effective solution for energy saving and emission reduction of inland ships, which have flexible and changeable working conditions. HPS has great advantages with its improved dynamic performance, lower fuel consumption and emission; however, there are some challenges for system energy distribution and power control due to the additional variables introduced into the energy conservation equation. To optimize the energy management strategy (EMS) and develop the potential of the HPS, a novel energy management strategy based on model predictive control (MPC) has been proposed for a parallel hybrid propulsion system, which combines a natural gas engine, lithium-ion batteries, and permanent magnet synchronous motor (PMSM). First, a speed predictor based on long short-time memory (LSTM) is developed to forecast vessel velocity within a specified range, that is a precise reference input of the EMS. The proposed strategy not only consider the short-term cost of natural gas consumption and pollutant emissions, but also take into account the long-term cost for the capacity degradation of lithium-ion batteries during navigation. Specifically, a tuning factor is introduced to balance the trade-off between the performance of emission and battery capacity decay. Finally, the effectiveness of the proposed strategy is verified by the simulation experiments and HIL test. The results demonstrate that compared with the rule-based (RB) strategy, the MPC energy management strategy proposed in this study can reduce fuel consumption by 0.71%, NOx and HC emissions by 15.18%, and the battery capacity degradation by 96.34% with the appropriate tuning factor. The proposed EMS not only improves the system efficiency and reduce the fuel consumption but also extend the service life of the battery system. The research confirms the beneficial effects of the HPS on reducing fuel consumption and emissions for inland ships, and provides a new idea for the HPS control and energy management.

1 INTRODUCTION

Increasing concerns about the global climate and fuel energy have made the transportation face higher challenges in improving energy efficiency and reducing emissions. Electrified propulsion systems offer a highly promising direction for energy conservation and emission reduction in the transportation sector, and have become a focal point in recent years. Inland waterway transportation vessels have also joined the trend, with several successful applications emerging. For instance, COSCO Shipping built a 700 TEU electric container ship in 2022, equipped with a battery capacity of 57600 kWh [1]. Another example is the “Three Gorges Hydrogen Boat No.1”, which utilizes a hybrid power system (HPS) combining a 500kW fuel cell and a lithium battery set of 1800 kWh, marking it as China’s first fuel cell powered vessel [2].

HPS is well adapted to the operating conditions of inland waterways vessels, owing to its efficiency, economic benefits, and power redundancy. Compared to traditional propulsion system, HPS offers significant advantages in handling frequent load demand fluctuations [3]. The integration of multiple energy sources offers significant advantages while increasing the complexity of system control. This complexity is mainly manifested in the expansion of the degrees of freedom for power allocation [4]. The energy management strategy (EMS) plays a pivotal role in this context, serving as the critical control mechanism for allocating instantaneous load demands among various power sources. The efficacy of the EMS directly determines the overall performance of the hybrid propulsion system, influencing key parameters such as energy efficiency, operational stability, and system reliability [5].

Dynamic programming (DP) algorithm is one of the most commonly used energy management strategies, with its core principle based on the Bellman optimality principle. It is capable of effectively determining the optimal operating parameters of the system under specified navigation conditions. However, the traditional DP algorithm suffers from the problem of “dimensional catastrophe” as the number of discrete grids increases. Moreover, its dependence on complete navigation condition information significantly limits its real-time applicability. An enhanced DP algorithm was proposed in Ref. [6] that effectively eliminates the need for interpolation operations during backward recursion and forward solving by reconstructing the state transfer equation as a functional expression of state variables. This approach removes the accumulated errors associated with interpolation, thereby improving the accuracy of the globally optimal solution. Additionally, the algorithm incorporates the level set method to constrain the control input. Pontryagin's minimum principle (PMP) and equivalent consumption minimization strategy (ECMS), as two typical real-time strategies, can be computed in real-time. PMP and ECMS are essentially equivalent and both capable of providing near-optimal solutions, but they still rely on global navigation information. In Ref. [7] the computational resources and uncertainty of driving conditions are both considered. An adaptive PMP strategy based on two-stage optimization was proposed to address uncertainties driving conditions in real-world environments. The first stage uses the available driving condition to derive the optimal trajectory for using PMP method. The state trajectory and optimal costate are transmitted to the inner loop, where the A-PMP is applied. The state of energy (SOE) is fed back to controller. When a deviation occurs between SOE and its optimal trajectory reference, the predictive costate is adjusted. Finally, the robustness and effectiveness of the EMS are verified in real vehicles. However, such a closed-loop operation can be more conveniently implemented in another real-time optimization method known as Model predictive control (MPC).

MPC processes the ability to handle optimization problems with multiple variables and constraints, and its inherent feedback control within the framework makes it particularly suitable for complex energy management in HPS. Several studies have already applied MPC to solve energy management problems of HPS. In Ref. [8] a variable weight decision model predictive control (VWDMPC) strategy was developed for HPS. This strategy achieves a balance between fuel consumption and dynamic performance. The optimization problem of energy management is simplified by clearly integrating the Karush-Kuhn-Tucker (KKT) conditions and weight adjustment process. Finally, the weight range balancing the economic and dynamic performance was determined. An online EMS based on economic model predictive control (EMPC) scheme was presented in [9]. What the innovation of this strategy is that a multiple objective cost function is proposed. All the cost terms including fuel consumption and battery degradation are expressed in monetary terms. The strategy was validated on the electric bus in the end. Furthermore, in Ref. [10], a hierarchical distributed MPC control method was proposed for HPS. The upper-level controller is responsible for formulating the global energy allocation strategy. The lower-level controller focuses on real-time optimization of individual subsystems. These studies demonstrate the role of MPC in improving energy efficiency.

The MPC repetitively solves optimal control problems with repeated update of state information. MPC calculates the optimal energy distribution within the prediction horizon. Therefore, the acquisition of reference trajectory is critically important, which is refer to future ship speed in energy management. There are various methods to predict future speed, such as, [11] utilized time series imaging technology for ship speed prediction. These ship speed prediction methods can be naturally integrated with the MPC strategy: the prediction module provides future speed information over a time horizon, and the MPC controller utilizes these predictions to compute the optimal energy allocation scheme. For instance, a strategy for fuel cell hybrid electric vehicle based on MPC-DP was proposed in [12], which incorporates a backpropagation (BP) neural network speed predictor. A bidirectional long short-term memory (Bi-LSTM) network was proposed for driving condition prediction in [13]. Similarly, an EMS combined working condition prediction was discussed in [14]. The results indicate that the MPC with Markov speed predictor has a better performance in economic efficiency than that without it. Therefore, integrating driving condition prediction with energy management is an effective approach to enhance energy efficiency.

The energy management problem of the HPS is a nonlinear optimization problem with multiple objectives and multiple constraints. In this work, an MPC-based EMS is discussed, which not only considers the fuel economy, but also takes into account the pollutant emissions and battery degradation. Cause a single metric will lead to an extreme performance on the other aspects of HPS, whereas a multi-objective approach can improve the overall performance. Moreover, a ship prediction model based on LSTM is introduced into the energy management framework. A tuning factor is introduced in the EMS to adjust the HPS performance between emissions and battery degradation. Therefore, the proposed strategy can balance the pollutant emissions and battery degradation while ensuring the economic efficiency. The implementation of MPC controller is achieved using the ACADO toolbox, which uses a special iteration scheme to shorten the computation time in order to achieve real-time control. In the end, to verify the effectiveness of the proposed strategy, simulation and HIL testing are conducted.

The structure of this paper is organized as follows. Section 2 presents the models of the considered system. Section 3 discusses the MPC-based energy management strategy and the speed predictor. Simulation and Hardware-in-Loop (HIL) results are demonstrated in Section 4. Finally, the conclusions are provided in Section 5.

2 System description and modelling

This work focuses on an inland ship equipped with a gas-electric parallel HPS, which comprises a natural gas engine (NGE), a fixed pitch ratio propeller, a lithium-ion battery set, and a permanent magnet synchronous motor (PMSM). Figure 1 illustrates the hybrid system. The propeller can be driven by NGE or PMSM, or a combination of both. Such a hybrid system fully takes advantage of the clean and efficient features of NGE and battery energy storage, significantly improving the energy efficiency of the ship. PMSM can improve the acceleration performance of NGE and compensate for its limitations in dynamic response characteristics. Compared with series system, the parallel system has fewer energy transfer paths and higher propulsion efficiency. The specifications of the HPS are shown in Table 1.

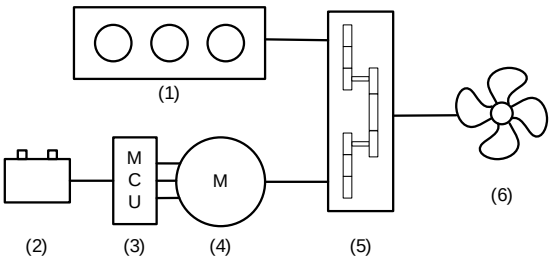

(1) Natural Gas Engine
(2) Battery Pack
(3) Motor Control Unit
(4) Permanent magnet synchronous motor
(5) Gear box
(6) Propeller

Figure 1. Gas-electric parallel HPS.

Table 1. Specifications of HPS powertrain.

Type	Item	Value	Unit
Natural gas engine	Maximum power	243	kW
	Maximum torque	1600	Nm
	Maximum rotational speed	1850	rpm
Battery pack	-	$LiFePO_4$	-
	Capacity	200	Ah
	Nominal voltage	576	V
PMSM	Maximum power	100	kW
	Maximum torque	850	Nm
	Maximum rotational speed	2200	rpm
Propeller	P/D	1.1	-
	Diameter	1.05	m
	Blade area ratio	0.4	-
Gearbox	Gear ratio	2.63:1	-

2.1 Natural gas engine model

A numerical model of the NGE is developed for energy management, incorporating gas consumption rate and pollutant emissions, specifically NOx and HC. Figures 2a and 2b depict the NGE gas consumption rate map and pollutant emission rate map, respectively. They are all expressed as a function of NGE speed N_{eng} and torque Q_{eng} as in Eqs. 1 and 2.

$$\dot{m}_f = f(N_{eng}, Q_{eng}) \tag{1}$$

$$\dot{m}_{emis} = g(N_{eng}, Q_{eng}) \tag{2}$$

Figures 3a and 3b present the simulation errors of the numerical model for the gas consumption map and emission map, respectively. The errors generally range between 5% and 10%, with large deviations observed in certain low-load regions. However, the polynomial model is consistent with the original maps in terms of change patterns, and the EMS tries to avoid NGE operating in low-load regions where higher gas consumption and emission costs are incurred. Thus, the model is considered feasible.

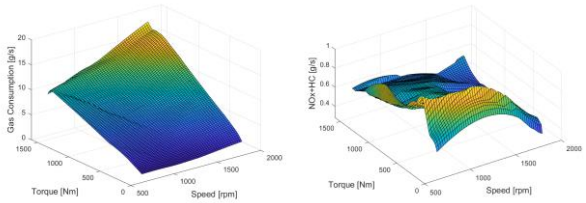

(a) (b)

Figure 2. (a) Gas consumption rate map, (b) NOx+HC emission map.

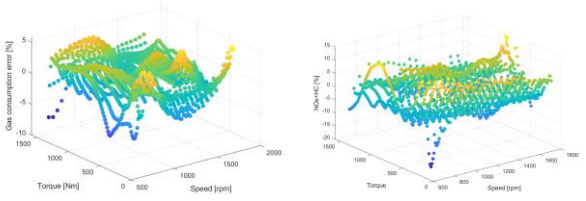

(a) (b)

Figure 3. (a) Gas consumption error, (b) NOx+HC emission error.

The dynamic behavior of the NGE speed can be derived from Eq. 3.

$$\frac{dN_{eng}}{dt} = \frac{30}{\pi J_{eng}}(Q_{mot} + Q_{eng} - Q_{load}) \tag{3}$$

$$Q_{load} = Q_{prop} / i_{gb} \tag{4}$$

where, J_{eng} is the moment of inertia of NGE; i_{gb} is the gearbox reduction ratio. Q_{load} is the propeller torque load Q_{prop} transmitted to the powertrain through the gearbox.

2.2 PMSM

PMSM is driven by the lithium battery set. As a propulsion motor, the PMSM is characterized by high efficiency and fast dynamic response. The charging and discharging efficiency of the battery is considered in this work, which can be expressed as a function of the battery output power in Eq. 5 [15].

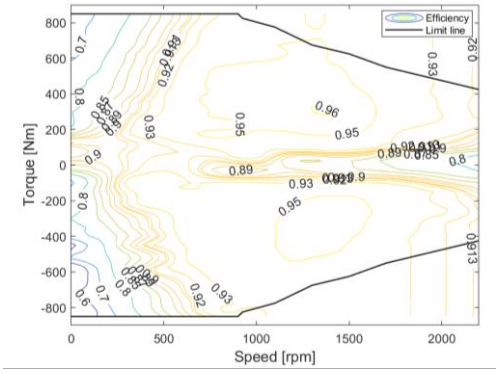

Figure 4. PMSM efficiency map.

$$\eta_{bat} = \eta_{bat,0} P_{bat}^2 + \eta_{bat,1} P_{bat} + \eta_{bat,2} \tag{5}$$

where, $\eta_{bat,i}$, $i = 1,2,3$ is fitting coefficients; P_{bat} is battery power.

Consequently, the efficiencies of the PMSM and the battery are combined using Eq. 6 to more accurately simulate the system. The battery output power can be calculated by Eq. 7. Figure 5 shows the output power map of the battery.

$$\eta_t(N_{mot}, Q_{mot}) = \begin{cases} \eta_{pmsm}\eta_{bat}, Q_{mot} \le 0 \\ 1/\eta_{pmsm}\eta_{bat}, Q_{mot} > 0 \end{cases} \tag{6}$$

$$P_{bat} = \omega_{mot} Q_{mot} \eta_t \tag{7}$$

2.3 Battery model

The energy storage battery is one of the important components of the propulsion system. To balance accuracy with computational efficiency, a Rint equivalent circuit model is established in this

work for simulating battery power and voltage dynamics. The battery open circuit voltage characteristics and internal resistance characteristics are presented in Figure 6, and the

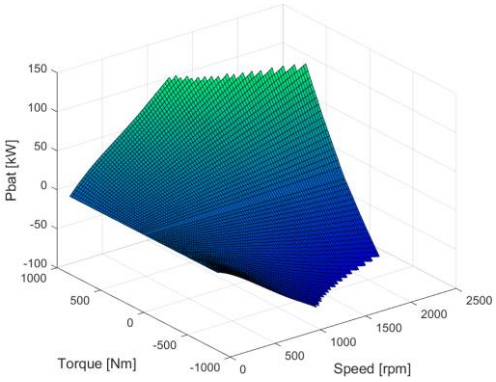

Figure 5. Battery output power map.

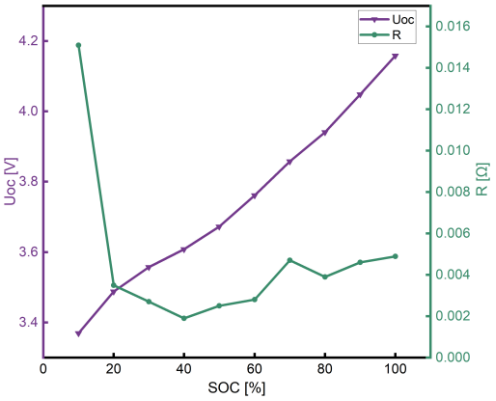

Figure 6. Battery cell characteristics of open-circuit voltage and internal resistance

state-of-charge (SOC) of the battery can be obtained by Eq. 8.

$$SOC = SOC_{ini} - \int_0^T \frac{P_{bat}}{Q_{bat}U_{bat}}dt \tag{8}$$

where, Q_{bat} is the battery capacity; U_{bat} is the terminal voltage. Battery degradation stems from electrochemical side reactions, including SEI growth and lithium loss, that persistently occur during normal operation. In this work, capacity reduction is adopted as the primary metric for assessing battery degradation. A semi-empirical model is employed to describe the battery life [16].

$$Q_{loss} = P(c)exp(-\frac{E_a(c)}{R_T T_b})A_h^{\ z} \tag{9}$$

where, Q_{loss} is the percentage of battery capacity loss; c is the current rate; A_h is the ampere-hour (Ah) throughput; z is a constant parameter determined by experiment; R_T is the ideal gas constant; T_b is the battery temperature; $E_a(c)$ is the activation energy; $P(c)$ is the pre-exponential factor; both $E_a(c)$ and $P(c)$ are function of current rate.

$$P(c) = \alpha_1 c^2 + \alpha_2 c + \alpha_3 \tag{10}$$

$$E(c) = 31370 - \beta c \tag{11}$$

with α_i, i =1,2,3 and β constant parameters.

Generally, the Q_{loss} reaches 20% signifies the end-of-life (EOL) for the battery, indicating that the battery should be retired from service [17]. The total Ah before EOL can be calculated using Eq. 12.

$$A_{h,eol} = [\frac{20}{P(c)exp(-\frac{E_a(c)}{RT})}]^{1/z} \tag{12}$$

In this case, the battery degradation in discrete-time domain Δq_{loss} can be quantified by Eq. 13.

$$\Delta q_{loss} = \frac{|I_b|\Delta t}{2 \times 3600 A_{h,eol}} \tag{13}$$

2.4 Propeller model

The generation of propeller thrust and torque involves complex hydrodynamic processes. Fitting formulas and semi-empirical Eqs 14 and 15 are utilized to calculate thrust T_p and torque Q_p [18].

$$T_p = K_T(J)\rho D^4 n_p^2 \tag{14}$$

$$Q_p = K_Q(J)\rho D^5 n_p^2 \tag{15}$$

$$n_p = \frac{N_{eng}}{60 i_{gb}} \tag{16}$$

where, K_T and K_Q are thrust coefficient and torque coefficient, respectively. They dependent on the advance ratio J and are typically obtained through open-water test. Additionally ρ is water density; D is the propeller diameter; n_p is propeller rotation speed in r/s.

2.5 Hull dynamics

Eq. 17 calculates the ship's speed.

$$\dot{V}_s = \frac{1}{m}(T_{ship} - R_{ship}) \tag{17}$$

where, V_s is the ship speed; m is the ship mass; T_{ship} represents the thrust, considering thrust deduction caused by hull-propeller interaction; R_{ship} is the ship resistance, which is related to V_s.

$$T_{ship} = T_p(1-t) \tag{18}$$

$$R_{ship} = c_r V_s^2 \tag{19}$$

where, t is thrust deduction factor; c_r is resistance coefficient.

3 EMS and control

This section discusses the establishment of a predictive energy management strategy based on MPC and a ship speed predictor. A multiple-objectives cost function that consists of gas consumption, emissions and battery degradation is formulated for MPC. The primary tasks of the MPC controller are to track the NGE reference speed and determine the optimal energy distribution, while ensuring that the NGE and PMSM work within their respective operational limits. Also an LSTM model based ship speed predictor is developed to provide reference information for MPC controller. Figure 7 illustrates the energy management framework for HPS.

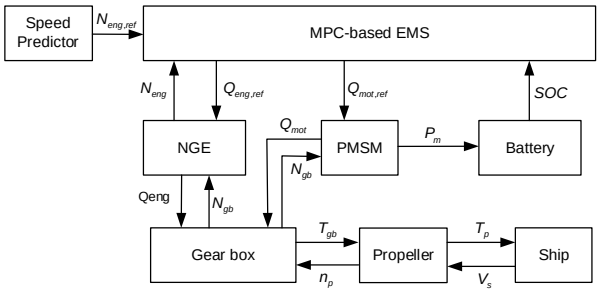

Figure 7. HPS energy management framework.

3.1 MPC-based EMS

The primary objective of the EMS is to minimize the total cost of system operation. Therefore, the multiple-objective cost function in this work incorporates gas consumption, NOx and HC emissions, and battery degradation, which are calculated using Eqs 20, 21, and 22, respectively.

$$\dot{J}_{fc} = \dot{m}_{fc} + \lambda_{eqv}\frac{P_{bat}}{H_u} \tag{20}$$

where, λ_{eqv} is the equivalent factor; H_u is the lower heating value of natural gas. In addition, both emissions and battery degradation are scaled to gas consumption for comparison within the same magnitude.

$$\dot{J}_{emis} = \frac{\dot{m}_{fc,max}}{\dot{m}_{emis,max}}\dot{m}_{emis} \tag{21}$$

$$\dot{J}_{bat} = \frac{\dot{m}_{fc,max}}{\dot{q}_{loss,max}}\dot{q}_{loss} \tag{22}$$

The energy management based on MPC is an optimal control problem (OCP) with an infinite number of optimization variables. In this work, the direct method is applied to transform such an OCP to a nonlinear program (NLP) problem [19]. Thus, the discretized cost function is given in Eq. 23.

$$\begin{aligned} J =& \| SOC(N_u) - SOC_{ref}(N_u) \|_{w_6}^2 + \\ & \sum_{k=1}^{N_u-1}\begin{bmatrix} \| N_{eng}(k) - N_{eng,ref}(k) \|_{w_1}^2 + \|J_{fc}(k)\|_{w_2}^2 + \\ (1-\mu)\|J_{emis}(k)\|_{w_3}^2 + \mu\|J_{bat}(k)\|_{w_4}^2 \end{bmatrix} \end{aligned} \tag{23}$$

where, N_u is the control horizon which is 40 in this work; $\| N_{eng}(k) - N_{eng,ref}(k) \|_{w_1}^2$ represents the stage cost of NGE speed tracking error. The subsequent three terms correspond to the stage costs associated with gas consumption, NOx and HC emissions, and battery degradation, respectively. The parameter μ is a tuning factor, which is adopted to balance the emissions against battery protection. The term $\| SOC(N) - SOC_{ref}(N) \|_{w_6}^2$ denotes the final cost of battery SOC variation, ensuring equality between initial and final SOC values. In the end, $w_i, i = 1,\ldots,6$ represents the weighting factors for each component.

In each control interval, the MPC solves such an NLP problem with constraints to obtain the control input that minimizes the specified cost J.

$$\begin{aligned} &\min_{Q_{eng},Q_{mot}} \quad J(N_{eng}, SOC, Q_{eng}, Q_{mot}) \\ &s.t.\ \ Eqs.\ 1-9,2 \\ &\quad SOC_{min} \le SOC \le SOC_{max} \\ &\quad N_{eng,min} \le N_{eng} \le N_{eng,max} \\ &\quad N_{mot,min} \le N_{mot} \le N_{mot,max} \\ &\quad 0 \le Q_{eng} \le Q_{eng,max}(N_{eng}) \\ &\quad Q_{mot,min}(N_{mot}) \le Q_{mot} \le Q_{mot,max}(N_{mot}) \end{aligned} \tag{24}$$

The constraints include limitations on SOC and speed operation range. The torque constraints of NGE and PMSM are obtained from their external characteristics.

To implement the MPC controller, a real-time iteration (RTI) scheme is adopted in this work [20]. Typically, the RTI is realized using a direct multiple shooting technology with sequential quadratic programming (SQP) [21]. In each control interval, the SQP performs only one iteration. As a result, the optimization problem does not iterate to convergence in each control cycle, but gradually converges through multiple control steps. The RTI carefully designs the preparation stage and feedback stage of the algorithm. In the preparation stage, the Gauss-Newton method is used to approximate the Hessian matrix. Once the system information is obtained, the feedback stage immediately calculates the solution of QP and outputs to the control plant. In this way, RTI can provide approximate optimal feedback control within a limited time, and approach the precise optimal solution as the iteration progresses. What's more, the strategy is finally implemented through the ACADO toolkit [22].

3.2 Ship speed predictor

The goal of energy management is to meet the needs of ship navigation while minimizing system costs. Under this condition, providing future speed information for the controller is extremely important for improving the efficiency of HPS. The ship's speed typically changes over time, and the current speed is closely related to the speed and environmental conditions of the past period. Therefore, the ship speed data can be processed as time series. In Ref. [23], a long short-term memory (LSTM) network was proposed for driving condition prediction. Thus, in this work, an LSTM model is used to predict the ship's future speed. The predicted results are then converted to engine speed by the propulsion system model, and input into the MPC controller to optimize the energy allocation of the HPS.

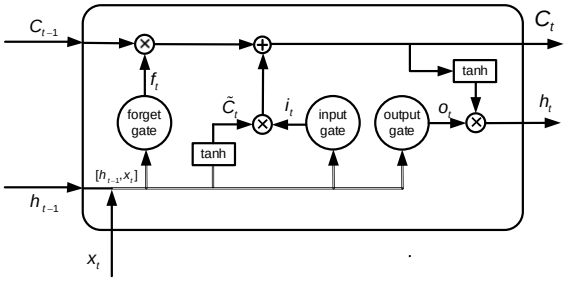

Figure 8. LSTM structure.

Figure 8 presents the structure of LSTM. The forget gate indicates the degree to which the previous cell information needs to be forgotten. The input gate determines the current input information entering the cell. The new cell state is composed of the previous cell state controlled by the forget gate and the new information controlled by the input gate. The output gate extracts useful information from the current cell information. These gates are typically sigmoid activation functions. The parameter transfer process of LSTM can be represented as Eq. 25.

$$\begin{cases} i_t = \sigma(w_{ix}x_t + w_{ih}h_{t-1} + b_i) \\ \tilde{C}_t = tanh(w_{cx}x_t + w_{ch}h_{t-1} + b_c) \\ f_t = \sigma(w_{fx}x_t + w_{fh}h_{t-1} + b_f) \\ o_t = \sigma(w_{ox}x_t + w_{oh}h_{t-1} + b_o) \\ C_t = f_t \bullet C_{t-1} + i_t \bullet \tilde{C}_t \\ h_t = o_t \bullet tanh(C_t) \end{cases} \tag{25}$$

where, σ is activation function; w and b donate weight and bias respectively; i_t, f_t, o_t, x_t, and C_t represent the input gate, forget gate, output gate, data input and cell state at the current moment, respectively. Moreover, $\tilde{C}_t$ and h_t represent the hidden layer information.

To train the speed predictor, real operational data of ships in the Yangtze River were collected. During the training process, Adam is used as the optimizer for deep learning. 80% of the dataset is used for training, and the remaining 20% for testing. The ship speed prediction results based on the LSTM method is shown in Figure 9. The results indicate that the predictions are relatively accurate and can meet the needs of energy management.

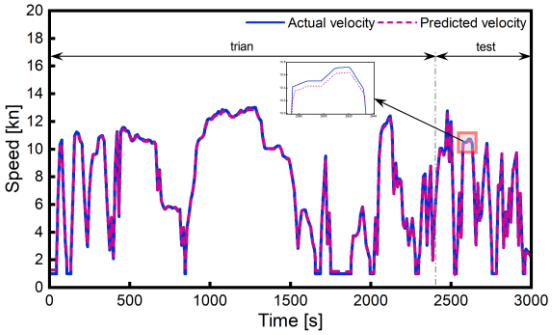

Figure 9. Ship speed prediction result.

4 Results and discussion

The results of MPC-based EMS are presented and discussed in this section, and the effectiveness of the EMS has been further validated through HIL testing. The test conditions in [24] are utilized to

configure the simulation environment. The working conditions in this study were extracted by machine learning and contained different working characteristics of the ship, that can provide more comprehensive testing for HPS.

4.1 Simulation results

Firstly, a moderate value is set for neutral tuning factor. The results of MPC strategy with μ =0.5 are presented in Figures 10 and 11. As a comparison, the results based on the DP strategy and the rule-based (RB) strategy are shown together. The DP strategy also considers a multiple-objective cost function $J_{fc}+(1-\mu)J_{emis}+\mu J_{bat}$ as the optimal benchmark for comparison. The RB strategy establishes the energy management rules according to SOC thresholds, with the economy of HPS as the main consideration objective.

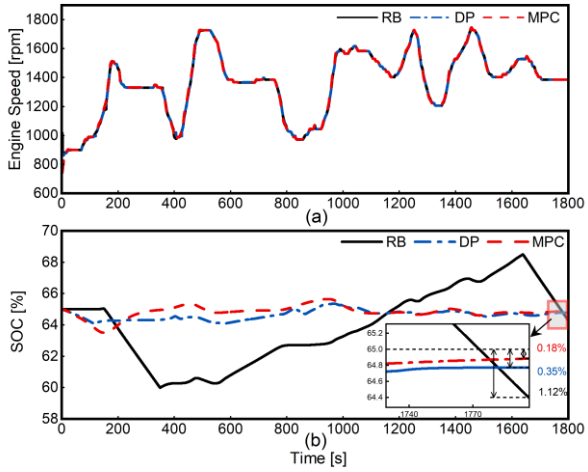

Figure 10. (a) NGE speed tracking, (b) SOC trajectory.

The results in Figure 10 indicate that all three control strategies satisfy the requirements for speed tracking and SOC maintenance. The final SOC values under different strategies are around 65% with a deviation within 5%.

In the configured working conditions, the period from 0 to 120s represents a low load region. During this stage, the ship's power demand is relatively low. As a result, both the MPC and DP strategies generate higher PMSM torque to prevent the NGE from operating under a low-efficiency region. As the power demand rapidly increases during sharp acceleration phase from 120 to 190s, the MPC strategy gradually reduces the PMSM torque to coordinate the acceleration process of the NGE. At 150s, the PMSM transitions to generating mode, and the NGE enters its high-efficiency zone. In contrast, under the DP strategy, the PMSM quickly switches to generating mode, driving the NGE into a high-load region to achieve better efficiency.

During the subsequent deceleration and constant speed phases from 190 to 400s, the MPC and DP strategies generate distinct energy allocation paths. The PMSM remains in generating

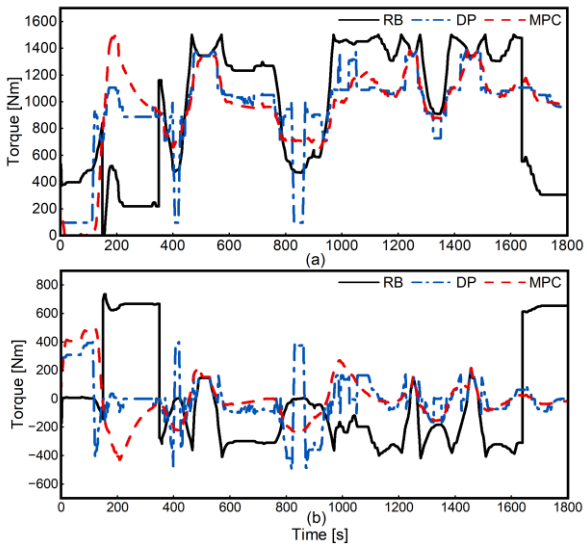

Figure 11. Torque distribution results under strategies, (a) torque of NGE, (b) torque of PMSM.

mode under the MPC strategy, supplying electrical energy to the battery while coordinating the torque output of NGE based on changes in demand power. This is due to the constraint of battery SOC change in the MPC strategy. However, under the DP strategy, almost all required power is fulfilled by NGE, while the torque of PMSM only experiences slight fluctuations around 0. This is because meeting the demand power by NGE reduces the secondary conversion of energy, resulting in higher system efficiency. What's more, the SOC under the DP strategy is relatively high at this time. In the similar working process between 400 and 900s, the opposite result occurs: under the MPC strategy, the NGE meets nearly all power demand, while in the DP strategy, the PMSM operates in generating mode to charge the battery. The torque distribution of the system under the RB strategy is relatively simple. In contrast, the torque distribution of the RB strategy is relatively straightforward. During the initial operation phase, the battery has sufficient energy, so the PMSM handles most of the load. When the ship's power demand increases significantly, the NGE is responsible for meeting the power demand. To ensure the NGE works along the predefined optimal operation curve, the PMSM either supplements the insufficient power or switches to generation mode to adjust the operating point of NGE.

In the power fluctuation phase from 900 to 1700s, MPC converges to the same result as DP. In this case, the PMSM mainly plays a role in torque coordination. As the required power demand increases, the electromagnetic torque is reduced to assist the NGE in acceleration. Conversely, when the required demand decreases, PMSM switches to power generation mode, on the one hand to replenish battery energy to maintain the SOC within normal range, and on the other hand to adjust the working point of NGE to improve economic efficiency and reduce emissions.

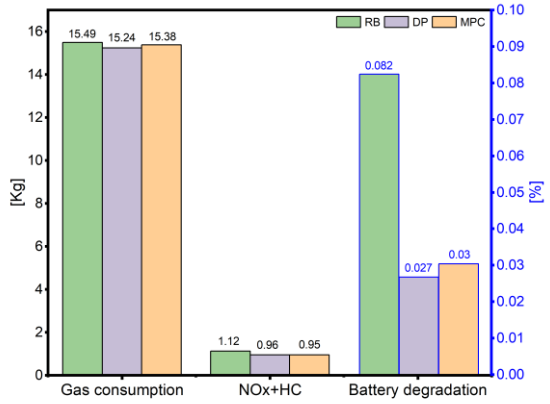

Figure 12. Results under three strategies.

Figure 12 shows the results of three strategies. Compared to the optimal DP strategy, MPC only has a 0.919% higher gas consumption but a 0.104% lower emission level. This difference is caused by the different working path of the NGE. In terms of battery degradation, MPC is 11.1% higher than DP. This phenomenon can be explained by Figure 13, which exhibits the operating points of the PMSM. The PMSM under MPC strategy operates more frequently in high-speed and high-load region, which leads to larger battery currents and consequently greater battery degradation. However, the MPC strategy achieves reductions of 0.71% in gas consumption, 15.18% in emissions and 96.34% in battery degradation compared to the RB strategy. In summary, the EMS based on MPC strategy is capable of satisfying the energy management requirements of HPS.

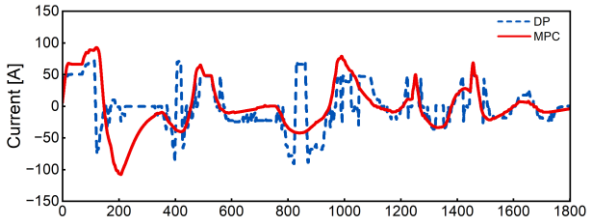

Figure 13. Battery output current.

In some situations, HPS may pay more attention to certain performance aspects. For example, when entering emission-restricted zones such as ports, the HPS may prefer to reduce the pollutant emissions, while during normal operation the battery degradation and gas consumption may be more focused.

Therefore, two additional simulation configurations, μ =0.2 and μ =0.8, are set up in this work, respectively representing emission optimization priority and battery degradation optimization priority. In order to compare the results clearly, the operating points of NGE and PMSM are placed on the gas consumption rate map, NOx and HC emission rate map and combined motor efficiency map. It can be seen that under the emission optimal strategy, to avoid low-efficiency region, the NGE starts output none-zero torque at alternating high speed. And in the subsequent operation, the NGE operates in a range where emissions are below 30 g/kWh, whereas under the battery degradation optimal strategy, it operates below 50 g/kWh. Moreover, under battery optimal strategy, PMSM reduces the output range to decrease the battery current, thereby delaying

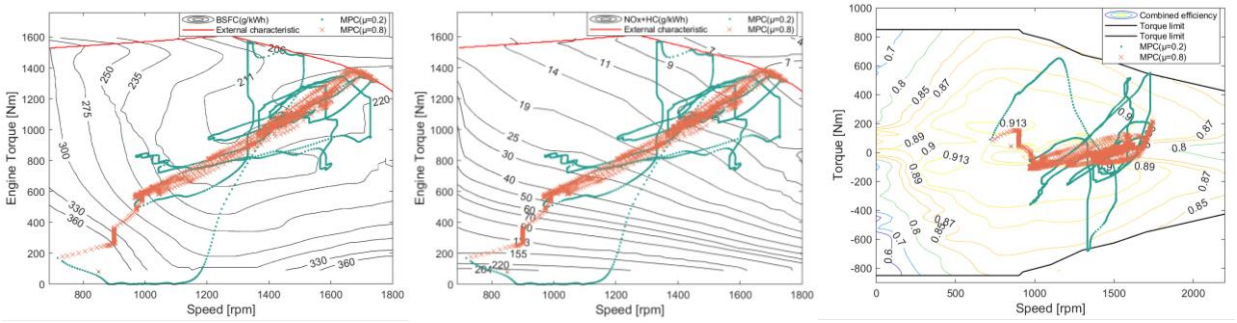

(a) (b) (c)

Figure 14. (a) NGE operating points with gas consumption rate map, (b) NGE operating points with emission rate map, (c) PMSM operating points with efficiency map.

degradation. In this scenario, the PMSM primarily plays a role in adjusting the operating conditions of the NGE. Thus, under μ =0.8 configuration, the reason why the NGE operates in a strip-shaped area can be explained. Because the fuel and emission efficiencies are guaranteed in this area. Table 2 shows the results under different tuning factors. Overall, the tuning factor has a significant impact on the optimization results of energy management.

Table 2. Results of different values of tuning factor.

		MPC	μ =0.2	μ =0.8
Gas consumption	[kg]	15.466	15.465
NOx+HC	[kg]	0.930	1.015
Battery degradation	[%]	0.054	0.013
Final SOC	[%]	64.99	64.87

4.2 Hardware-in-loop test

In this work, the proposed EMS is further validated through HIL testing. An HIL test environment was established using the NI CompactRIO-9038 platform. The simulation model and the MPC strategy were deployed to the chassis of cRIO-9038 through a code generation tool. Additionally, NI-9021 and NI-9263 modules were utilized to collect model feedback states and output control commands from EMS, respectively. Figure 15 illustrates this process. And Figure 16 shows the physical hardware setup.

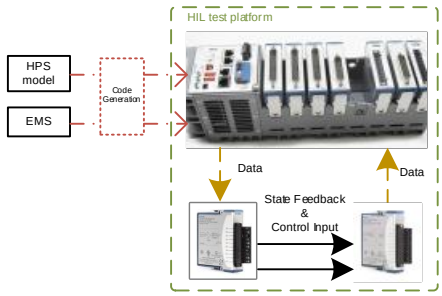

Figure 15. The deployment process of HIL test.

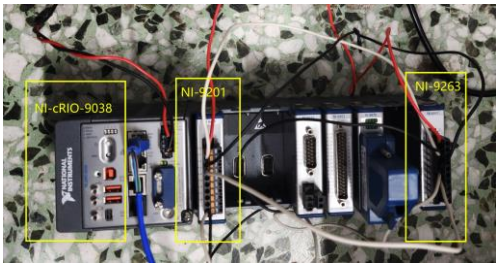

Figure 16. NI cRIO-9038 with NI-9021 and NI-9263 models.

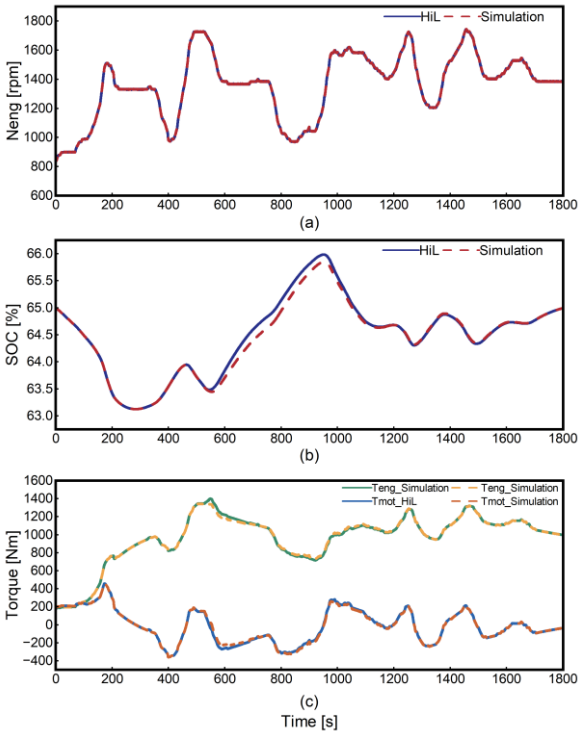

Figure 17. Results of HIL test.

The HIL results present in Figure 17 are basically the same as those of simulation, which can effectively meet the requirements for speed tracking and battery SOC constraints. Due to the HIL calculation accuracy, slight differences in torque distribution can be observed between 530~670s. However, these errors are within an acceptable range and have little impact on the results. The HIL results are shown in Table 3, which don't have a significantly difference compared to simulation results. Thus, the real-time performance of the proposed strategy has been successfully validated.

Table 3. Comparison of HIL and simulation results.

		HIL	Simulation
Gas consumption	[kg]	15.453	15.452
NOx+HC	[kg]	1.002	1.000
Battery degradation	[%]	0.040	0.039
Final SOC	[%]	64.99	64.99

5 Conclusions

In order to solve the optimal control problem of gas-electric parallel marine hybrid propulsion system, a predictive EMS based on MPC was proposed. The main task of EMS was to achieve power allocation under multiple objectives, including gas consumption, emissions and battery degradation. And a tuning factor was introduced to change the performance preferences of HPS.

Additionally, a ship predictor based on LSTM model was utilized.

The effectiveness of the proposed EMS has been validated through simulation and HIL test. The MPC-based EMS reduced gas consumption, pollutant emissions and battery degradation by 0.71%, 15.18% and 96.34%, respectively, compared to the RB strategy. In addition, its performance closely approximates the optimal results of the DP strategy. Furthermore, the tuning factor operates within the expected range, effectively determining the trade-off performance between emissions and battery protection in the HPS. The proposed strategy demonstrates high efficiency and significant application potential.

6 Acknowledgments

This work was supported by the Youth Fund of the National Natural Science Foundation of China (52401371)

7 References and bibliography

[1] Feng Y, Dai L, Yue M, et al. Assessing the decarbonization potential of electric ships for inland waterway freight transportation[J]. *Transportation Research Part D*: *Transport and Environment*, 2024, 129: 104151.

[2] Wang Z, Dong B, Wang Y, et al. Analysis and evaluation of fuel cell technologies for sustainable ship power: Energy efficiency and environmental impact[J]. *Energy Conversion and Management: X*, 2024, 21: 100482.

[3] Damian S E, Wong L A, Shareef H, et al. Review on the challenges of hybrid propulsion system in marine transport system[J]. *Journal of Energy Storage*, 2022, 56: 105983.

[4] Serrao L, Onori S, Rizzoni G. A comparative analysis of energy management strategies for hybrid electric vehicles[J]. 2011.

[5] Guo X, Lang X, Yuan Y, et al. Energy management system for hybrid ship: Status and perspectives[J]. *Ocean Engineering*, 2024, 310: 118638.

[6] Xu C, Fan L, Jiang Z, et al. Investigation on energy management strategy of gas-electric marine hybrid propulsion system with improved dynamic programing algorithm[J]. I*nternational Journal of Engine Research*, 2024, 25(1): 140-155.

[7] Schmid R, Buerger J, Bajcinca N. Energy management strategy for plug-in-hybrid electric vehicles based on predictive PMP[J]. IEEE Transactions on Control Systems Technology, 2021, 29(6): 2548-2560.

[8] Sun X, Yao C, Song E, et al. Novel enhancement of energy distribution for marine hybrid propulsion systems by an advanced variable weight decision model predictive control[J]. *Energy*, 2023, 274: 127269.

[9] Pozzato G, Müller M, Formentin S, et al. Economic MPC for online least costly energy management of hybrid electric vehicles[J]. *Control Engineering Practice*, 2020, 102: 104534.

[10] Liu H, Fan A, Li Y, et al. Hierarchical distributed MPC method for hybrid energy management: A case study of ship with variable operating conditions[J]. *Renewable and Sustainable Energy Reviews*, 2024, 189: 113894.

[11] Jiang X, Dai Y, Li S, et al. Research on ship speed prediction based on time series imaging and deep convolutional network fusion method[J]. *Applied Ocean Research*, 2025, 154: 104384.

[12] Liu C, Li X, Chen Y, et al. Real-time energy management strategy for fuel cell/battery vehicle based on speed prediction DP solver model predictive control[J]. *Journal of Energy Storage*, 2023, 73: 109288.

[13] Chatterjee D, Biswas P K, Sain C, et al. Bi-LSTM predictive control-based efficient energy management system for a fuel cell hybrid electric vehicle[J]. *Sustainable Energy, Grids and Networks*, 2024, 38: 101348.

[14] Hao J, Ruan S, Wang W. Model predictive control based energy management strategy of series hybrid electric vehicles considering driving pattern recognition[J]. *Electronics*, 2023, 12(6): 1418

[15] Kalikatzarakis M, Geertsma R D, Boonen E J, et al. Ship energy management for hybrid propulsion and power supply with shore charging[J]. *Control Engineering Practice*, 2018, 76: 133-154.

[16] Zhang Y, Zhang C, Fan R, et al. Twin delayed deep deterministic policy gradient-based deep reinforcement learning for energy management of fuel cell vehicle integrating durability information of powertrain[J]. *Energy Conversion and Management*, 2022, 274: 116454.

[17] Perez H E, Hu X, Dey S, et al. Optimal charging of Li-ion batteries with coupled electro-thermal-aging dynamics[J]. *IEEE Transactions on Vehicular Technology*, 2017, 66(9): 7761-7770.

[18] Smogeli Ø N. Control of marine propellers: from normal to extreme conditions[J]. 2006.

[19] Yang S. A Trust-Region Method for Multiple Shooting Optimal Control[J]. 2022.

[20] Diehl M, Bock H G, Schlöder J P. A real-time iteration scheme for nonlinear optimization in optimal feedback control[J]. *SIAM Journal on control and optimization*, 2005, 43(5): 1714-1736.

[21] Diehl M, Bock H G, Schlöder J P. A real-time iteration scheme for nonlinear optimization in optimal feedback control[J]. *SIAM Journal on control and optimization*, 2005, 43(5): 1714-1736.

[22] Houska B, Ferreau H J, Diehl M. ACADO toolkit—An open‐source framework for automatic control and dynamic optimization[J]. *Optimal control applications and methods*, 2011, 32(3): 298-312.

[23] Song K, Huang X, Xu H, et al. Model predictive control energy management strategy integrating long short-term memory and dynamic programming for fuel cell vehicles[J]. *International Journal of Hydrogen Energy*, 2024, 56: 1235-1248.

[24] Sun X, Gao Y, Zhang Q, et al. Machine Learning-Based Extraction Method for Marine Load Cycles with Environmentally Sustainable Applications[J]. *Sustainability*, 2024, 16(11): 4840